An MR Radiomics Framework for Predicting the Outcome of Stereotactic Radiation Therapy in Brain Metastasis*

Elham Karami, Mark Ruschin, Hany Soliman, Arjun Sahgal, Greg J. Stanisz, and Ali Sadeghi-Naini, *Senior Member, IEEE*

Abstract— **Despite recent advances in cancer treatment, patients with brain metastasis still suffer from poor overall survival (OS) after standard treatment. Predicting the treatment outcome before or early after the treatment can potentially assist the physicians in improving the therapy outcome by adjusting a standard treatment on an individual patient basis. In this study, a data-driven computational framework was proposed and investigated to predict the local control/failure (LC/LF) outcome in patients with brain metastasis treated with hypo-fractionated stereotactic radiation therapy (SRT). The framework extracted several geometrical and textural features from the magnetic resonance (MR) images of the tumour and edema regions acquired for 38 patients. Subsequent to a multi-step feature reduction/selection, a quantitative MR biomarker consisting of two features was constructed. A support vector machine classifier was used for outcome prediction using the constructed MR biomarker. The bootstrap .632+ and leave-one-patient-out cross-validation methods were used to assess the model's performance. The results indicated that the outcome of LF after SRT could be predicted with an area under the curve of 0.80 and a cross-validated accuracy of 82%. The results obtained implied a good potential of the proposed framework for local outcome prediction in patients with brain metastasis treated with SRT and encourage further investigations on a larger cohort of patients.**

I. Introduction

Brain metastasis is the most common intracranial malignancy. The treatment options of brain metastasis include whole-brain radiation therapy (WBRT), stereotactic radiation therapy (SRT), surgical resection, and systemic therapy. SRT has now become the standard treatment method for patients having less than 10 brain lesions, as it is associated with less brain damage compared to WBRT[1].

Recent clinical practices performed for cancer treatment suggest that the therapy outcome can be significantly improved by tailoring the treatment methods to the individual patient's characteristics [2]. In fact, an appropriate personalized treatment method can minimize the complications and morbidity caused by a futile treatment. The standard procedure of radiation treatment planning for brain metastasis involves magnetic resonance (MR) and computed tomography (CT) imaging. The former is used for segmenting the regions of interest (ROIs), and the latter is used for radiation therapy simulation and deriving the radiation dose maps. MR images are also acquired after the treatment as part of the standard follow-up assessment that is mainly based on the changes in physical measurements of the tumour. However, such physical changes may not be evident on standard follow-up images until many months after the treatment. Also, due to a local recurrence, the tumour size may increase again several months after the treatment despite a detectable reduction in size early after the treatment.

Radiomics refers to high-throughput mining of medical images that applies data-driven computational methods to extract and explore quantitative biomarkers from medical images for specific diagnostic and/or prognostic applications. Such biomarkers often include geometrical and textural features of a region of interest (ROI) within the tissue, *e.g.*, a lesion or tumour. Geometrical features describe the morphology and shape of the ROI, whereas the textural features characterize the intra-ROI heterogeneity. Such features have demonstrated diagnostic and prognostic value in different clinical applications [3]–[8]. The application of radiomics in diagnosis and therapy response prediction has been investigated for several cancer types including breast, lung, and head and neck [8]–[17]. In these studies, various radiomic features are extracted from different imaging modalities including MRI, CT, and ultrasound. The previous studies have demonstrated that quantitative imaging features and, in particular, textural biomarkers have a high potential for cancer characterization in diagnostic and prognostic applications and implied that radiomics can serve as a bridge between medical imaging and personalized cancer therapeutics.

In this work, the potential of the MR radiomic features was investigated for predicting the local control/local failure (LC/LF) outcome in patients with brain metastasis treated with hypo-fractionated SRT. Several radiomic features were

*This Research was supported by Natural Sciences and Engineering Research Council (NSERC) of Canada, Canadian Institutes for Health Research (CIHR), and Terry Fox Foundation.

E. Karami is with the Department of Medical Biophysics, University of Toronto, Toronto, ON, Canada; also with the Physical Sciences Platform, Sunnybrook Research Institute, Sunnybrook Health Sciences Centre, Toronto, ON, Canada (e-mail: elham.karami@sri.utoronto.ca).

M. Ruschin, H. Soliman, and A. Sahgal are with the Department of Radiation Oncology, Odette Cancer Centre, Sunnybrook Health Sciences Centre, Toronto, ON, Canada; also with the Department of Radiation Oncology, University of Toronto, Toronto, ON, Canada (e-mail: mark.ruschin@sunnybrook.ca; hany.soliman@sunnybrook.ca; arjun.sahgal@sunnybrook.ca).

G. Stanisz is with the Department of Medical Biophysics, University of Toronto, Toronto, ON, Canada; also with the Physical Sciences Platform, Sunnybrook Research Institute, Sunnybrook Health Sciences Centre, Toronto, ON, Canada (e-mail: stanisz@sri.utoronto.ca)

A. Sadeghi-Naini is with the Department of Electrical Engineering and Computer Science, York University, Toronto, ON, Canada; also with the Department of Radiation Oncology and Physical Sciences Platform, Odette Cancer Centre and Sunnybrook Research Institute, Sunnybrook Health Sciences Centre, Toronto, ON, Canada; also with the Department of Medical Biophysics, University of Toronto, Toronto, ON, Canada (e-mail: asn@yorku.ca; phone: 416-736-2100 x20590).

978-1-5386-1311-5/19/$31.00 ©2019 IEEE

extracted from MR images of 38 patients diagnosed with brain metastasis and planned for SRT. The features were analyzed through a multi-step feature reduction/selection process with cross-validation that resulted in an optimal MR biomarker consisting of two features. A support vector machine (SVM) classifier was used to predict the outcome of the patients in terms of LC/LF using the optimal MR biomarker. The classification results demonstrated that early changes in the optimal MR biomarker after the SRT can predict the 6-month LC/LF outcome of a tumour with cross-validated sensitivity and specificity of 84% and 79%, respectively.

II. Methods

A. Dataset

This study was conducted in accordance with institutional research ethics board approval from Sunnybrook Health Sciences Centre (SHSC), Toronto Canada. Imaging and clinical data were collected from 38 patients diagnosed with brain metastasis and treated with hypo-fractionated SRT. All patients were diagnosed with a single tumour, and the dataset included a total of 38 malignant lesions. The imaging data consisted of gadolinium contrast-enhanced T1-weighted (T1w), and T2-weighted-fluid-attenuation-inversion-recovery (T2-FLAIR) images acquired immediately before (baseline) and within three months (first follow-up) after the treatment. Both datasets were acquired as part of the institutional standard of care for brain metastasis treatment. The in-plane image resolution was 0.5 mm for both T1w and T2-FLAIR images. The slice thickness was 1.5 mm and 5 mm for T1w and T2-FLAIR images, respectively. The 6-month LC/LF outcome for each lesion was determined by a radiation oncologist and neuroradiologist using the follow-up imaging data acquired about 6 months after the treatment.

B. Tumour/Edema Mask Generation

The treatment planning data consisted of the tumour contours delineated by expert oncologists on T1w images (Fig. 1(a)). In order to segment the edema, first the T2-FLAIR images were registered on T1w using an affine registration with mutual information (MI) as the similarity metric [18]. Next, the edema was segmented on the registered images using a region growing algorithm followed by manual refinement under the supervision of an expert oncologist. Finally, the tumour and edema masks were warped on original T2-FLAIR images using the inverse of the registration transformation matrix. A similar procedure was performed on the follow-up images to obtain the tumour and edema masks. The mask generation pipeline was implemented in ITK software toolkit while the manual adjustments were performed using 3D Slicer software package [19].

C. Feature Extraction

The extracted features consisted of two groups of geometrical and textural features. The geometrical features describing the ROI shape were obtained from the 2D axial slices of the tumour and edema masks (Fig. 1(b)), and subsequently averaged over all 2D slices. The geometrical features included the area, perimeter, circle metric, aspect-ratio, convexity, eccentricity, solidity, and extent of the segmented region.

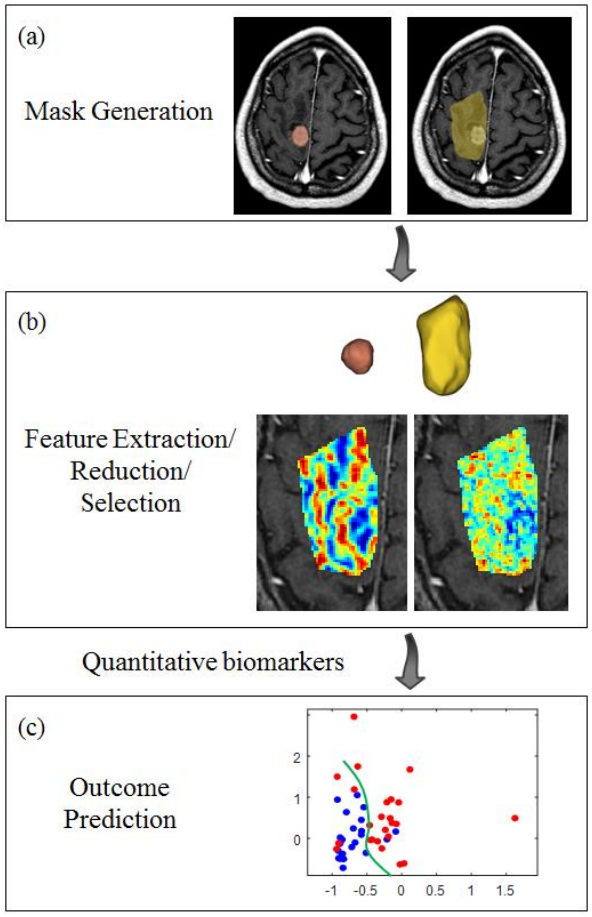

Figure 1. The MR radiomics framework for prediction of radiotherapy LC/LF outcome in metastatic brain tumours.

The textural features were extracted from both T1w and T2-FLAIR images within the tumour and edema masks separately. The textural features included the first order features derived from the image histogram [20], as well as the second order features derived from the accumulated gray-level-cooccurrence-matrix (GLCM) of the image with a neighborhood parameter of 1 to 4 voxels [21]. The first order histogram features describe the distribution of the voxel intensities, while the second order GLCM features depict the inter-dependency or co-occurrence of two voxels at specific relative position (Fig. 1(b)). Another set of textural features applied in this study were the histogram features derived from the Local Binary Pattern (LBP) [22] parametric images. A total of 220 quantitative features were explored in this study. All features were extracted from both the baseline and first follow-up images and the relative change from the baseline at the first follow-up was used for outcome prediction (Fig. 1(c)).

III. Results

A. Biomarker Discovery

The features extracted from the tumour and edema regions, were first assessed using a Pearson correlation analysis to exclude the highly correlated features. Fig. 2(a) depicts the R^2 heat map obtained from the Pearson correlation matrix for all the features.

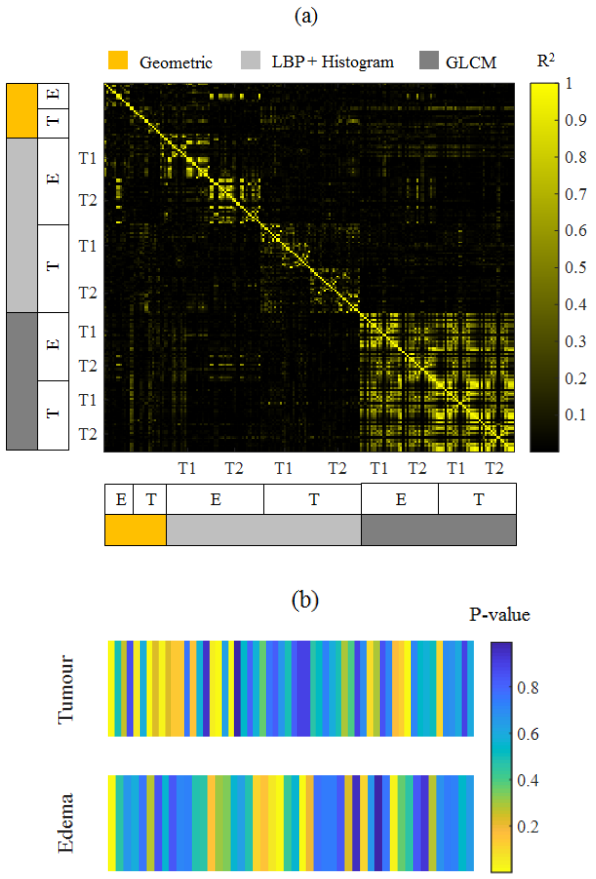

Figure 2. (a) The R^2 heat map demonstrating the correlation between the features. (b) The p-value heat map for the quantitative MR features extracted from the tumour and edema regions.

As shown in Fig. 2(a), the highly correlated features formed several clusters. Therefore, the R^2 matrix was thresholded for values greater than 0.80 to identify the clusters of highly-correlated features. Next, each cluster was reduced to a single representative feature with the largest dynamic range. The correlation analysis reduced the number of features from 220 to 106.

Subsequent to the feature reduction, the level of statistical difference exhibited by each feature between the lesions with an LC versus LF outcome was assessed using a Mann Whitney U test with a critical p-value of 0.05 for feature selection. Fig. 2(b) demonstrates the distribution of p-values for features extracted from tumour and edema, respectively. The feature selection procedure consisted of two steps. First, a sub-optimal set of features was ranked using the p-values obtained from the Mann Whitney U test in conjunction with a leave-one-out sampling scheme. At each sampling step, the p-values were calculated over the 37 selected lesions. Next,

TABLE I. THE SELECTED FEATURES FOR THE OPTIMAL MR BIOMARKER.

Outcome	Optimal Features	p-value
6-month LC/LF	Edema_Geometric_Solidity_T2	0.006
	Edema_LBP_Median_T1	0.02

TABLE II. THE LC/LF OUTCOME PREDICTION RESULTS.

Outcome	$\widehat{AUC}_{.632+}$	Accuracy	Sensitivity	Specificity
6-month LC/LF	0.80	82%	84%	79%

from all the features having a p-value smaller than 0.05, the first 15 features with the smallest p-values were identified. Finally, the features were ranked based on their frequency of occurrence in the best 15 features over the 38 sampling folds. The feature ranking step was followed by a forward selection scheme based on the area under the curve (AUC) with bootstrap .632+ ($\widehat{AUC}_{.632+}$) to select the features forming an optimal MR biomarker for outcome prediction [23]. The selected features are listed in Table I. As the table implies, the features included in the optimal MR biomarker are corresponding to the edema region.

B. Outcome Prediction

An SVM classifier with a Gaussian kernel was applied to predict the LC/LF outcome of each lesion using the optimal MR biomarker. The model performance was assessed using both the $\widehat{AUC}_{.632+}$, and a leave-one-patient-out (LOPO) cross validation scheme. The results have been summarized in Table II. An $\widehat{AUC}_{.632+}$ of 0.80 was obtained for predicting the radiation therapy outcome using the optimal MR biomarker. The optimal biomarker could also predict the LC/LF outcome of the stereotactic radiation therapy with a LOPO cross-validated sensitivity, specificity, and accuracy of 84%, 79%, and 82%, respectively.

IV. DISCUSSION

In this study, an MR radiomics framework was proposed and investigated to predict the 6-month LC/LF outcome of hypo-fractionated SRT for patients with brain metastasis. A total of 220 geometrical and textural features were extracted from the T1w and T2-FLAIR images within the tumour, and edema regions. A multi-step feature reduction/selection scheme was used to find the optimal quantitative MR biomarker for LC/LF outcome prediction. The optimal biomarker consisted of two features extracted from the edema region. The bootstrap .632+ and LOPO cross-validation methods were used to assess the potential of the optimal MR biomarker for outcome prediction. The results indicated that the optimal MR biomarker can predict the 6-month LC/LF outcome of hypo-fractionated SRT with an $\widehat{AUC}_{.632+}$ = 0.80, and accuracy = 82%.

In conclusion, the results obtained from this study demonstrated that the quantitative biomarkers extracted from T1w and T2-FLAIR images have a good potential to predict the LC/LF outcome of SRT early after the treatment. Such prediction can facilitate effective treatment adjustments on an individual patient basis before it is potentially too late. Further investigations are required to evaluate the efficacy of these biomarkers on a larger cohort of patients, and to compare the performance of the proposed radiomics framework with other methods such as convolutional neural networks.

REFERENCES

[1] M. Yamamoto, T. Serizawa, T. Shuto, A. Akabane, Y. Higuchi, J. Kawagishi, K. Yamanaka, Y. Sato, H. Jokura, S. Yomo, O. Nagano, H. Kenai, A. Moriki, S. Suzuki, Y. Kida, Y. Iwai, M. Hayashi, H. Onishi, M. Gondo, M. Sato, T. Akimitsu, K. Kubo, Y. Kikuchi, T. Shibasaki, T. Goto, M. Takanashi, Y. Mori, K. Takakura, N. Saeki, E. Kunieda, H. Aoyama, S. Momoshima, and K. Tsuchiya, "Stereotactic radiosurgery for patients with multiple brain metastases (JLGK0901): a multi-institutional prospective observational study," *Lancet. Oncol.*, vol. 15, no. 4, pp. 387–95, Apr. 2014.

[2] D. S. Haslem, S. B. Van Norman, G. Fulde, A. J. Knighton, T. Belnap, A. M. Butler, S. Rhagunath, D. Newman, H. Gilbert, B. P. Tudor, K. Lin, G. R. Stone, D. L. Loughmiller, P. J. Mishra, R. Srivastava, J. M. Ford, and L. D. Nadauld, "A Retrospective Analysis of Precision Medicine Outcomes in Patients With Advanced Cancer Reveals Improved Progression-Free Survival Without Increased Health Care Costs," *J. Oncol. Pract.*, vol. 13, no. 2, pp. e108–e119, 2017.

[3] R. J. Gillies, P. E. Kinahan, and H. Hricak, "Radiomics: Images Are More than Pictures, They Are Data," *Radiology*, vol. 278, no. 2, pp. 563–577, 2016.

[4] A. Heindl, S. Nawaz, and Y. Yuan, "Mapping spatial heterogeneity in the tumor microenvironment: a new era for digital pathology," *Lab. Investig.*, vol. 95, no. 4, pp. 377–84, Apr. 2015.

[5] R. Natrajan, H. Sailem, F. K. Mardakheh, M. Arias Garcia, C. J. Tape, M. Dowsett, C. Bakal, and Y. Yuan, "Microenvironmental Heterogeneity Parallels Breast Cancer Progression: A Histology-Genomic Integration Analysis," *PLoS Med.*, vol. 13, no. 2, p. e1001961, Feb. 2016.

[6] K. Polyak, "Heterogeneity in breast cancer," *J. Clin. Invest.*, vol. 121, no. 10, pp. 3786–8, Oct. 2011.

[7] H. Tadayyon, L. Sannachi, A. Sadeghi-Naini, O. Falou, M. L. Oelze, and G. J. Czarnota, "Quantitative ultrasound monitoring of breast cancer cell death in vivo using tissue-scattering models – a preclinical study," in *38th International Symposium on Ultrasonic Imaging and Tissue Characterization (UITC)*, 2013.

[8] D. Sengupta and G. Pratx, "Imaging metabolic heterogeneity in cancer," *Mol. Cancer*, vol. 15, p. 4, 2016.

[9] M. J. Gerdes, A. Sood, C. Sevinsky, A. D. Pris, M. I. Zavodszky, and F. Ginty, "Emerging understanding of multiscale tumor heterogeneity," *Front. Oncol.*, vol. 4, p. 366, 2014.

[10] H. Tadayyon, A. Sadeghi-Naini, and G. J. Czarnota, "Noninvasive characterization of locally advanced breast cancer using textural analysis of quantitative ultrasound parametric images," *Transl. Oncol.*, vol. 7, no. 6, pp. 759–767, Dec. 2014.

[11] R. T. H. M. Larue, G. Defraene, D. De Ruysscher, P. Lambin, and W. Van Elmpt, "Quantitative radiomics studies for tissue characterization: A review of technology and methodological procedures," *British Journal of Radiology*, vol. 90, no. 1070. pp. 1–10, 2017.

[12] H. Tadayyon, L. Sannachi, M. J. Gangeh, C. Kim, S. Ghandi, M. Trudeau, K. Pritchard, W. T. Tran, E. Slodkowska, A. Sadeghi-Naini, and G. J. Czarnota, "A priori prediction of neoadjuvant chemotherapy response and survival in breast cancer patients using quantitative ultrasound," *Sci. Rep.*, vol. 7, p. 45733, 2017.

[13] H. J. W. L. Aerts, E. R. Velazquez, R. T. H. Leijenaar, C. Parmar, P. Grossmann, S. Cavalho, J. Bussink, R. Monshouwer, B. Haibe-Kains, D. Rietveld, F. Hoebers, M. M. Rietbergen, C. R. Leemans, A. Dekker, J. Quackenbush, R. J. Gillies, and P. Lambin, "Decoding tumour phenotype by noninvasive imaging using a quantitative radiomics approach," *Nat. Commun.*, vol. 5, 2014.

[14] A. Sadeghi-Naini, H. Suraweera, W. T. Tran, F. Hadizad, G. Bruni, R. F. Rastegar, B. Curpen, and G. J. Czarnota, "Breast-Lesion Characterization using Textural Features of Quantitative Ultrasound Parametric Maps," *Sci. Rep.*, vol. 7, p. 13638, 2017.

[15] W. T. Tran, M. J. Gangeh, L. Sannachi, L. Chin, E. Watkins, S. G. Bruni, R. F. Rastegar, B. Curpen, M. Trudeau, S. Gandhi, M. Yaffe, E. Slodkowska, C. Childs, A. Sadeghi-Naini, and G. J. Czarnota, "Predicting breast cancer response to neoadjuvant chemotherapy using pretreatment diffuse optical spectroscopic texture analysis," *Br. J. Cancer*, vol. 116, no. 10, pp. 1329–1339, 2017.

[16] M. J. Gangeh, H. Tadayyon, L. Sannachi, A. Sadeghi-Naini, W. T. Tran, and G. J. Czarnota, "Computer Aided Theragnosis Using Quantitative Ultrasound Spectroscopy and Maximum Mean Discrepancy in Locally Advanced Breast Cancer," *IEEE Trans. Med. Imaging*, vol. 35, no. 3, pp. 778–790, 2016.

[17] A. Sadeghi-Naini, L. Sannachi, H. Tadayyon, W. T. Tran, E. Slodkowska, M. Trudeau, S. Gandhi, K. Pritchard, M. C. Kolios, and G. J. Czarnota, "Chemotherapy-Response Monitoring of Breast Cancer Patients Using Quantitative Ultrasound-Based Intra-Tumour Heterogeneities," *Sci. Rep.*, vol. 7, p. 10352, 2017.

[18] D. L. G. Hill, P. G. Batchelor, M. Holden, and D. J. Hawkes, "Medical image registration," *Physics in Medicine and Biology*, vol. 46, no. 3. pp. 173–178, 2001.

[19] A. Fedorov, R. Beichel, J. Kalpathy-Cramer, J. Finet, J. C. Fillion-Robin, S. Pujol, C. Bauer, D. Jennings, F. Fennessy, M. Sonka, J. Buatti, S. Aylward, J. V. Miller, S. Pieper, and R. Kikinis, "3D Slicer as an image computing platform for the Quantitative Imaging Network," *Magn. Reson. Imaging*, vol. 30, no. 9, pp. 1323–1341, 2012.

[20] N. Aggarwal and R. K. Agrawal, "First and Second Order Statistics Features for Classification of Magnetic Resonance Brain Images," *J. Signal Inf. Process.*, vol. 03, no. 02, pp. 146–153, 2012.

[21] R. M. Haralick, K. Shanmugam, and I. Dinstein, "Textural Features for Image Classification," *IEEE Trans. Syst. Man. Cybern.*, vol. 3, no. 6, pp. 610–621, Nov. 1973.

[22] D. C. He and L. Wang, "Texture Unit, Texture Spectrum, and Texture Analysis," *IEEE Trans. Geosci. Remote Sens.*, vol. 28, no. 4, pp. 509–512, 1990.

[23] B. Sahiner, H.-P. Chan, and L. Hadjiiski, "Classifier performance prediction for computer-aided diagnosis using a limited dataset," *Med. Phys.*, vol. 35, no. 4, pp. 1559–70, Apr. 2008.